

## **Simplified 1D Empirical Model for Volumetric Behavior of High-Carbonate Clay**

Vázquez-Boza, Manuel; Justo Alpañés, José Luis; Durand, Percy; Delgado Trujillo, Antonio; Justo Moscardó, Enrique (2019). International Journal of Geomechanics, (19) 4: 04019018.

This is the final Draft Manuscript.

This material may be downloaded for personal use only. Any other use requires prior permission of the American Society of Civil Engineers. This material may be found at <https://ascelibrary.org/doi/10.1061/%28ASCE%29GM.1943-5622.0001359>

# 1 **A simplified 1-D empirical model for volumetric behaviour of high carbonate clay**

2  
3 Manuel Vázquez-Boza, Ph.D.<sup>1</sup>; José Luis Justo, Ph.D.<sup>2</sup>; Percy Durand, Ph.D.<sup>3</sup>; Antonio Delgado,  
4 Ph.D.<sup>4</sup>; and Enrique Justo, Ph.D.<sup>5</sup>.

5 <sup>1</sup>*Department of Building Structures and Ground Engineering, E.T.S Architecture, University of Seville,*  
6 *Spain (corresponding author). E-mail: [mboza@us.es](mailto:mboza@us.es).*

7 <sup>2</sup>*Professor Emeritus, Department of Building Structures and Ground Engineering, E.T.S Architecture,*  
8 *University of Seville; President, Royal Academy of Sciences of Seville, Spain. E-mail: [jlj@us.es](mailto:jlj@us.es).*

9 <sup>3</sup>*Department of Building Structures and Ground Engineering, E.T.S Architecture, University of Seville,*  
10 *Spain. E-mail: [percy@us.es](mailto:percy@us.es).*

11 <sup>4</sup>*Department of Building Structures and Ground Engineering, E.T.S Architecture, University of Seville,*  
12 *Spain. E-mail: [antoniodelga@us.es](mailto:antoniodelga@us.es).*

13 <sup>5</sup>*Department of Building Structures and Ground Engineering, E.T.S Architecture, University of Seville,*  
14 *Spain. E-mail: [ejem@us.es](mailto:ejem@us.es).*

15  
16 **Abstract:** The Guadalquivir blue marl is a high plasticity overconsolidated carbonate clay. This soil  
17 presents an elevated fragility and high susceptibility to moisture changes. These characteristics have caused  
18 many geotechnical accidents, such as the Aznalcollar dam failure, in Seville (Spain). A comprehensive test  
19 campaign has been conducted to determine the physical and chemical properties of the blue marl. Analysis  
20 by scanning electron microscopy (SEM) and mercury intrusion porosimetry (MIP) allowed characterising  
21 its internal structure, revealing clear differences between the macro and the microstructure. A novel model  
22 for predicting the volumetric deformation (under oedometric conditions) of the Guadalquivir blue marl with  
23 suction and vertical pressure changes has been proposed. The model, based on data from shrink-swell tests,  
24 provides an acceptable estimation of the volumetric behaviour of the soil with a relatively simple set of  
25 parameters. The results were experimentally verified by suction-controlled oedometer tests and showed an  
26 acceptable agreement with the data measured. It has been specified when swelling, shrinkage or collapse  
27 occur.

29 **Author keywords:** Blue marl, Volumetric deformation, 1D model, Suction, Unsaturated soil,  
30 Guadalquivir River.

31

## 32 **Introduction**

33 The bedrock layer of the Guadalquivir River basin consists of a plastic, carbonated and overconsolidated  
34 clay, known as Guadalquivir blue marl. For geotechnical purposes, the thickness of this layer can be  
35 considered infinite. Although the blue marl is normally found in deep strata, it emerges superficially in  
36 some areas of the provinces of Huelva, Seville, Córdoba and Jaén (Tsige 1999).

37 This geological formation, of marine origin, was deposited in the Upper Miocene (Tortonian). The  
38 geotechnical characteristics of the blue marl include expansive behaviour, highly fragile shear strength and  
39 degradation after drying and wetting cycles, particularly in the shallowest zones (Alonso and Gens 2006a;  
40 Galera et al. 2009). These characteristics have caused significant damages to structures, pavements, dams  
41 and other constructions. Particularly remarkable are the slide at Almodóvar del Río, which damaged the  
42 Seville-Madrid high speed railway, and the Aznalcóllar dam failure, that caused one of the greatest  
43 environmental disasters in Spain's recent history (Alonso and Gens 2006a; Alonso and Gens 2006b; Gens  
44 and Alonso 2006; Zabala and Alonso 2011). The cost of repairing and mitigation measures associated with  
45 the problematic characteristics of the Guadalquivir blue marl (especially due to its expansive character) can  
46 be estimated at 28 million euros per year, affecting a total population of six million people (Llorente 1986).

47 For these reasons, predicting the deformational behaviour of this soil is a research topic of particular  
48 interest. In this paper, the effect of suction changes on the volumetric behaviour of the blue marl is analysed.  
49 A one-dimensional (1-D) model to predict the deformational behaviour of this type of soil, valid for swell  
50 and shrinkage strains, is presented.

51 Techniques for estimating the 1-D behaviour of expansive soils have been of great interest to academics  
52 and practitioners since they provide valuable information using a simple formulation, which makes them  
53 especially useful for engineering practice applications (Vanapalli and Lu 2012).

54 One of the first methods to estimate deformation changes with suction was proposed by Aitchison  
55 (1973) who established a linear relationship between volumetric strain and suction change in logarithmic  
56 scale, controlled by a coefficient called instability index ( $I_{pt}$ ).

$$57 \quad \varepsilon_v = I_{pt} \cdot \log(\Psi_f / \Psi_i) \quad (1)$$

58 where  $\varepsilon_v$  is the volumetric strain (positive for compression), and  $\Psi_f$  and  $\Psi_i$  are the final and initial suctions.

59 Similar expressions were presented by McKeen (1980), based on previous work by Lytton (1977),  
60 Hamberg and Nelson (1984) and Dhowian (1990), using different names for the instability index. In some  
61 cases, the instability index was obtained through the COLE (Coefficient of Linear Extensibility) test  
62 developed by the US Soil Conservation Service (Brasher et al. 1966), the core shrinkage test (Mitchell and  
63 Avalle 1984) or indirectly through physicochemical parameters, such as the activity of clay or the cation  
64 exchange capacity (Pousada 1984).

65 Fredlund (1983) developed a model to predict the vertical displacements of the expansive soil of Regina  
66 (Canada). His formulation is also linear and relates the vertical displacements of the soil ( $\Delta H$ ) to the  
67 difference between the final effective pressure ( $\sigma'_f$ ) and the swelling pressure ( $p'_s$ ) in a logarithmic scale.

68

$$69 \quad \Delta H = C_s \cdot \frac{H}{1+e_0} \cdot \log\left(\frac{\sigma'_f}{p'_s}\right) \quad (2)$$

70

71 where  $H$  is the thickness of the soil layer that has the potential to heave and  $C_s$  is the swelling index.

72

73 Fityus and Smith (1998) performed oedometric tests to a clay from Newcastle (Australia) under  
74 overburden pressure under the assumption that a given variation in soil moisture produces a unique variation  
75 of deformation ratio, and generated a model (Eq. 7) valid for expansive and collapsing behaviour. In their  
76 model, the soil deformation was calculated as a function of the moisture increment through a linearity  
77 coefficient called volume change index ( $I_v$ ), that was shown to have a linear relationship with the vertical  
78 pressure applied in the test.

79

$$80 \quad \Delta H = -0.33 \cdot H \cdot I_v \cdot (w_f - w_i) \quad (3)$$

81

82 In this expression,  $w_f$  and  $w_i$  are the final and initial gravimetric moisture respectively,  $H$  is the thickness  
83 of the soil layer analysed and  $\Delta H$  is the vertical displacement in response to moisture change.

84 Vanapalli *et al.* (2010) proposed a model to evaluate the strain  $\varepsilon$  under oedometric conditions of  
85 expansive soils after moisture changes, based on Eq. (2):

86

$$\Delta H = C_s \cdot \frac{H}{1+e_0} \cdot \log \left( \frac{K \cdot \sigma'_{f_1}}{10 \left( \frac{I_{p1}}{C_s} \Delta w \right)} \right) \quad (4)$$

88

89 In this equation  $\Delta w$  is the moisture change, and  $K$  is a correction coefficient. The authors collected  
 90 information from numerous expansive soil tests in order to correlate  $K$ ,  $C_s$  and  $I_{p1}$  with the plasticity index  
 91 ( $I_p$ ). More recently, Tu and Vanapalli (2016) improved the model, including the relationship between  
 92 deformation and the soil water content curves (SWCC) of expansive soils from different locations.

93 Puppala *et al.* (2014) developed a very simple model to predict the swelling or shrinkage deformation  
 94 experienced by a clayey soil in response to moisture content change. Their method, based on previous work  
 95 by Kodikara and Choi (2006), established a linear relationship between the axial, radial and volumetric  
 96 strains and the water content change:

97

$$\varepsilon_{swell-shrink} = -\alpha \cdot \Delta w \quad (5)$$

99

100 where  $\varepsilon_{swell-shrink}$  is the swelling or shrinkage deformation (volume, axial or radial),  $\alpha$  is a proportionality  
 101 coefficient and  $\Delta w$  is the gravimetric moisture change.

102 To validate the model, Puppala *et al.* (2014) analysed the displacements measured at various sites in  
 103 Texas (USA), comparing the results obtained using Eq. 5 with commonly used models for the prediction  
 104 of deformation such as Lytton (1977) and also with a finite element (FEM) solution. The model produced  
 105 similar results to the FEM simulation and both of them showed acceptable agreement with the measured  
 106 deformations.

107 Despite the wealth of available simple methods in the literature to predict the volume change of  
 108 expansive soils, the majority of them cannot be used in all geotechnical situations, due to some limitations:  
 109 (a) most are valid for swelling, but not for shrinkage or collapse; (b) almost all use disturbed samples,  
 110 instead of undisturbed samples; and (c) most do not consider a wide range of vertical pressures. In Table 1,  
 111 a synthesis of the main characteristics of the 1-D methods analysed is presented.

112 Alonso *et al.* (1989) proposed a very complete 3-D formulation for unsaturated soils of low activity, the  
 113 BBM method that has won wide acceptance. Later Gens and Alonso (1992) extended it to the behaviour of  
 114 unsaturated expansive clays; the authors state that “it is likely that as further and more comprehensive  
 115 experimental data become available more complex versions of the framework will have to be used”. Both

116 methods lead to very sophisticated constitutive models based upon plenty of constants and experiments that  
117 were mostly carried out on compacted soils. They are models that should be used in very important  
118 geotechnical engineering situations, but the simplified method presented here may be used in many cases  
119 with sufficient level of accuracy.

120 The research presented in this paper aims to develop a simplified model to predict the deformational  
121 behaviour under oedometric conditions of the Guadalquivir blue marl. The model proposed is valid for the  
122 simulation of simple swelling, shrinkage and collapse conditions. It has been derived empirically with tests  
123 on undisturbed samples, applying a wide range of vertical pressures. The method has been validated with  
124 experimental results in suction-controlled oedometer cells.

125 These characteristics of the new model, prediction of swelling, shrinkage and collapse strains, use of  
126 undisturbed samples and application of different vertical loads, have not been considered in any of the  
127 simplified models analysed in Table 1.

128

## 129 **Soil characterisation. Physical, chemical and hydraulic properties**

130 The undisturbed samples used in this research were obtained from rotary boreholes located at different sites  
131 in the Guadalquivir river valley. The samples were collected from the zone of depth 5 to 35 m of the sites,  
132 which is the depth range of interest for engineering projects. The borehole locations are indicated in in Fig.  
133 1.

134 The use of undisturbed samples results in a greater dispersion of the experimental data, but provides  
135 more accurate information about the real behaviour of the natural soil. Preserving the moisture content and  
136 inner structure of the blue marl samples was considered crucial in this study because the shrink and swell  
137 behaviour of this type of soil is known to depend greatly on its microstructure (Tsige 1999).

138 The physical characterisation of the blue marl was done through the following tests: 76 natural moisture  
139 contents, 67 dry unit weights, 36 unit weights of solid particles, 33 Atterberg limits, 36 wet sieving and 10  
140 sedimentation analyses. The average results of the laboratory tests are shown in Table 2.

141 The soil was classified as high plasticity clay with CH classification according to the Unified Soil  
142 Classification System (USCS). The average soil properties shown in Table 2 are within the range of the  
143 values obtained by other authors for undisturbed samples of blue marl (Tsige 1999; Alonso and Gens 2006a;

144 Galera et al. 2009). It can be observed that the dispersion of physical properties is not very high, which  
145 allows considering the Guadalquivir blue marl as a single geotechnical unit.

146 The chemical and mineralogical composition of the soil are presented in Table 3. The samples showed  
147 a high carbonate content, with an average value of  $30.6 \pm 2.8\%$ . The mineralogical composition of the  
148 samples was determined by X-ray diffraction analysis. An oriented-aggregate analysis was used to  
149 differentiate the constituent minerals of the phyllosilicates.

150 The phyllosilicates species found in the marl samples are smectite, illite and kaolinite. The percentage  
151 of smectite (showing the highest dispersion in Table 3) is greater in areas near the soil surface and tends to  
152 diminish at higher depths, reaching a sustained value of around 2% at depths of around 35 meters. As for  
153 the rest of the phyllosilicates, their content remains approximately constant with depth.

154 The carbonate content increases slightly with depth and shows similar values to the ones reported by  
155 Galera et al. (2009) for depths of up to 100 m. As the soil dries, the carbonate particles tend to migrate from  
156 the inside of the sample towards the surface, where they precipitate forming nodules.

157 The content of calcite, quartz and dolomite remain constant with depth. The soil plasticity varies slightly  
158 with depth, reaching plasticity index values between 30 and 34 (Galera et al. 2009).

159 The microstructure of the blue marl has been analysed by the scan electron microscopy technique (SEM)  
160 and by mercury intrusion porosimetry (MIP) (Vázquez-Boza et al., 2014), showing a flocculated matrix  
161 where a macro and a microstructure can be clearly differentiated. In Fig. 2 and Fig. 3, two types of pores  
162 can be observed: intra-aggregate pores, with a size of 0.02 microns, and inter-aggregate pores, with sizes  
163 around 200 microns.

164 The relationship between gravimetric moisture and suction was established through the soil water  
165 characteristic curve (SWCC) of the soil. The points of the SWCC were obtained experimentally, using (a)  
166 the pressure membrane method for lower suction values ( $<1,000$  kPa) (Richards 1941; Bocking and  
167 Fredlund 1980) and (b) the dew point psychrometer for suctions greater than 1,000 kPa (Gee et al. 1992;  
168 Bullut et al. 2002; Leong et al. 2003). A single curve (Fig. 4) was obtained using samples from different  
169 sites. Then, the curve was approximated with a mathematical model.

170 The initial suction was measured with the filter paper method, according to ASTM D5298-94 (1994).  
171 Seven different measurements, from a single site (site A) and different depths, yielded an average value of  
172  $\psi_0 = 850$  kPa with little scattering. The points in the SWCC curve were obtained from samples with the  
173 initial suction that were then subjected to wetting and drying paths.

174 Several authors have obtained mathematical expressions for modelling the SWCC of an unsaturated  
 175 soil, although in some cases (e.g., Van Genuchten, 1980) the procedure to determine the parameters  
 176 required has been considerably complex. By contrast, the method presented by Fredlund and Pham (2006)  
 177 is simpler to implement and provides a good agreement with experimental data. For these reasons, this has  
 178 been the method selected to obtain the SWCC of the Guadalquivir blue marl.

179 In this model, the SWCC was approximated by three straight lines that fitted the experimental data in  
 180 the zones of low, medium and high suction respectively (Eq. 6).

181

$$\begin{aligned}
 182 \quad w_1(\Psi) &= w_u - S_1 \cdot \log(\Psi) & 1 \leq \Psi < \Psi_{\text{aev}} \\
 183 \quad w_2(\Psi) &= w_{\text{aev}} - S_2 \cdot \log(\Psi/\Psi_{\text{aev}}) & \Psi_{\text{aev}} \leq \Psi < \Psi_r \\
 184 \quad w_3(\Psi) &= S_3 \cdot \log(10^6/\Psi) & \Psi_r \leq \Psi \leq 10^6 \text{ kPa}
 \end{aligned} \tag{6}$$

185

186 Where  $w_u$  is the saturation moisture,  $w_{\text{aev}}$  and  $\Psi_{\text{aev}}$  are the air entry point moisture and suction,  $\Psi_r$  is the  
 187 residual suction and  $S_1, S_2, S_3$  are three linearity coefficients.

188 For the Guadalquivir blue marl, the parameters of Eq. (10) take the following values:  $w_u = 31\%$ ,  $w_{\text{aev}} =$   
 189  $29\%$ ,  $\Psi_{\text{aev}} = 180 \text{ kPa}$ ,  $w_r = 4.1\%$  and  $\Psi_r = 80 \text{ MPa}$ . Replacing these values in Eq. (6), the linearity coefficients  
 190  $S_1, S_2$  and  $S_3$  are obtained. In this way, the Fredlund and Pham (2006) formulation is particularised to the  
 191 case of the Guadalquivir blue marl as follows:

192

$$\begin{aligned}
 193 \quad w_1(\Psi) &= 35 - 2.66 \cdot \log(\Psi) & 1 \text{ kPa} \leq \Psi < 180 \text{ kPa} \\
 194 \quad w_2(\Psi) &= 29 - 9.4 \cdot \log(\Psi/180) & 180 \text{ kPa} \leq \Psi < 80000 \text{ kPa} \\
 195 \quad w_3(\Psi) &= 3.74 \cdot \log(10^6/\Psi) & 80000 \text{ kPa} \leq \Psi \leq 10^6 \text{ kPa}
 \end{aligned} \tag{7}$$

196

197 In Fig. 4, the experimentally measured values of water content and suction are compared with those  
 198 obtained from Eq. (7).

## 199 **Experimental investigations and results**

### 200 *Shrink-swell test*

201

202 The shrink-swell test combines the outcomes of two tests: a core shrinkage test and a swelling under  
203 load test (Mitchell and Avalle 1984; Cameron 1989; Fityus et al. 2005).

204 The core shrinkage test is performed on an undisturbed cylindrical sample with a diameter of 45 to 50  
205 mm and a height of 1.5-2 diameters. The test specimen is initially measured and weighed before being  
206 subjected to an air-drying process until its weight has stabilised. During this process the specimen is  
207 measured and weighed periodically. After finishing the air drying process, the sample is oven dried at a  
208 temperature between 105° and 110°. After at least 24 hours, the sample is again measured and weighed to  
209 determine the maximum volume loss and dry weight. This procedure allows obtaining the initial moisture  
210 content and the moisture content associated with each of the volume measurements taken during the  
211 process.

212 The swelling test is also performed on an undisturbed sample, placed in an oedometric ring of 45-50  
213 mm diameter and 20 mm height. The ring is mounted in a conventional oedometer with porous plates at the  
214 top and bottom of the sample, and loaded with 25 kPa vertical pressure. Thereafter, the sample is flooded.  
215 After 24 hours, the swelling strain is measured. The moisture contents at the beginning and the end of the  
216 test are determined.

217 The outcomes of the shrink-swell test, shown in Fig. 5, are a combination of the shrinking strains and  
218 swelling strains measured in the two respective tests. As can be observed, there is a moisture limit beyond  
219 which the shrinking deformations are stabilised at their maximum value, at the end of the core-shrinkage  
220 test. This value is called the shrink limit ( $w_{sh}$ ). Similarly, the final value of moisture content at the end of  
221 the swell test, once the swelling strains are stabilised, is called the swell limit ( $w_{sw}$ ).

222 In this study a total of five shrink-swell tests have been performed on undisturbed samples of the  
223 Guadalquivir blue marl, extracted at depths of 6.6, 18 and 21 meters from the same site (site A). The results  
224 of these tests are shown in Table 4.

225 In this table,  $w_{sw}$  and  $w_{sh}$  are the swell limit and the shrink limit, respectively,  $\varepsilon_{shver}$  and  $\varepsilon_{shvol}$  are the  
226 vertical and volumetric strains obtained in the core shrinkage test and  $\varepsilon_{sw}$  is the vertical strain in the swelling  
227 under load test. According to these results, the tests yielded an average value of 32.6% for the swell limit  
228 and 5.2% for the shrink limit. The average ratio between the vertical and volumetric strain in the core  
229 shrinkage test was 0.48.

230 The results from shrink-swell tests (particularly the values of the swell and shrink limits) and also from  
231 suction-controlled oedometric tests (as shown in the next section) constitute the basis of the empirical model

232 proposed in this paper, which will enable predicting the deformational behaviour in response to suction  
233 change of this type of plastic soil with a high carbonate content.

234

### 235 **Suction-controlled oedometer tests**

236

237 The volumetric behaviour in oedometric conditions of the blue marl samples was investigated with an  
238 oedometer cell (Fig. 6) designed in the Polytechnic University of Catalonia (Hoffmann et al. 2005). This  
239 cell allows imposing suction on the soil specimen by means of the axis translation, osmosis and vapour  
240 transfer techniques.

241 In the oedometer tests performed in this study the vapour transfer technique was chosen, using an NaCl  
242 solution for low suctions and a CaCl<sub>2</sub> solution for high suctions. A diaphragm pump was used to force  
243 vapour recirculation in the closed-loop (Villar 2000; Tang and Cui 2005). The experimental setup is shown  
244 in Fig. 6. All tests were carried out in a chamber at a temperature of  $20 \pm 0.5$  °C and a controlled humidity  
245 of  $70 \pm 5\%$ .

246 Due to the low permeability of the soil, the time to achieve suction equilibrium was very long. To  
247 estimate the equilibrium time, four undisturbed marl samples were tested in a pressure membrane apparatus.  
248 Two samples were wetted from the initial suction to a suction of 400 kPa, while the other two were dried  
249 from the initial suction to a suction of 1000 kPa. During the process, the samples were weighed periodically  
250 (every two days) until a steady value of the weight indicated that the suction equilibrium had been reached.  
251 The average equilibrium time for both the wetting and the drying paths was found to be 13 days.  
252 Nevertheless, a minimum duration of 15 days was established for the suction-controlled oedometric tests  
253 in order to guarantee that the suction equilibrium is indeed achieved.

254 The experimental programme carried out in the suction-controlled oedometer, including the applied  
255 suctions and pressure values, is shown in Table 5. The suction was applied at the beginning of each test and  
256 maintained during the test when the pressure changes were imposed. All the tests were performed on  
257 different samples of blue marl extracted from the same borehole, at a depth of 18 m.

258 The test results are shown in Fig. 7. It can be observed that the material becomes stiffer when the suction  
259 is increased, while for suctions lower than the initial suction the soil shows a clear expansive behaviour  
260 (tests EDO-SUC-1, EDO-SUC-2 y EDO-SUC-3).

261 For suctions under the initial suction the samples experienced swelling strains when the pressure applied  
262 was lower than 100 kPa. This value of the vertical pressure is very close to the swelling pressure of the  
263 material (75 kPa) that was determined through an oedometer test according to UNE 103602:1996.

## 264 **Model for 1D volumetric deformation**

265 From the results of the suction-controlled oedometer tests a correlation can be established between the  
266 volumetric deformation (under oedometric conditions) and the suction change (in a logarithmic scale) for  
267 the different values of vertical pressure applied in the tests.

268 Fig. 8 plots the evolution of the volumetric strain against the logarithm of the normalised suction  
269 ( $\Psi_f / \Psi_0$ ), where  $\Psi_f$  and  $\Psi_0$  are the final and initial suctions respectively for each vertical pressure applied.  
270 The data have been obtained from Fig. 7 and Table 5. This figure shows the idealized trajectories  
271 corresponding to the two vertical pressures of 50 and 400 kPa (that can be extrapolated to the rest of the  
272 vertical pressures), corresponding to the patterns of behaviour described in the following paragraphs.

273 It can be observed that for suctions under a certain limit, the strain remains constant. This limit coincides  
274 with the point called the swell limit ( $w_{sw}$ ) in the shrink-swell test. For the Guadalquivir blue marl this point  
275 represents an average water content of 32.6%, which corresponds to a suction of  $\Psi_{sw} \sim 10$  kPa according to  
276 the SWCC (Fig. 4).

277 In the high suction range, all the tested samples have experienced shrinking strains, that stabilise after  
278 a certain limit value of the suction. The soil water content corresponding to the final shrinking strain  
279 coincides with the shrink limit ( $w_{sh}$ ) calculated in the shrink-swell test. The average value of  $w_{sh}$  in the soil  
280 specimens tested was 5.2%, which corresponds to a suction of  $\Psi_{sh} \sim 80$  MPa (Fig. 4).

281 In the intermediate range of suctions between the swell and the shrink limit the soil strain is  
282 approximately proportional to the logarithm of suction, following a linear relationship that can be fitted  
283 with Eq. (1). The slope of this relationship corresponds to the instability index ( $I_{pt}$ ) in the Aitchison model.  
284 The values of  $I_{pt}$  obtained empirically for the different pressures applied in the oedometer tests are listed in  
285 Table 6. If  $I_{pt}$  is drawn as a function of the the applied vertical pressure, a clear correlation can be observed,  
286 which can be modeled as a linear regression (Fig. 9a). From this figure, the swelling pressure  $p_s=149$  kPa  
287 is the vertical pressure corresponding to a zero instability index, and so to no volume change under suction  
288 changes. In Figure 9b, the value of the instability index has been drawn in a more compact form as indicated  
289 in eq. (8):

290

291  $I_{pt}(\sigma_{vf}) = C \log\left(\frac{p_s}{\sigma_{vf}}\right)$  (8)

292 where  $C$  is a constant. For this particular soil  $C=0.023$  and  $p_s=149$  kPa.

293 The volumetric deformation under oedometric conditions can be expressed as:

294

295  $\varepsilon_v(\Delta\sigma_v, \Delta\Psi) = \varepsilon_v(\Delta\sigma_v, \Psi_0) + \varepsilon_v(\sigma_{vf}, \Delta\Psi)$  (9)

296

297 where  $\varepsilon_v(\Delta\sigma_v, \Delta\Psi)$  is the deformation corresponding to a simultaneous increment of vertical pressure ( $\Delta\sigma_v$ )

298 and suction ( $\Delta\Psi$ );  $\varepsilon_v(\Delta\sigma_v, \Psi_0)$  is the deformation caused by an increment of vertical pressure while keeping

299 the suction constant ( $\Psi_0$ ); and  $\varepsilon_v(\sigma_{vf}, \Delta\Psi)$  is the deformation experienced when an increment of suction is

300 applied at constant vertical pressure ( $\sigma_{vf}$ ).

301 The value of  $\varepsilon_v(\Delta\sigma_v, \Psi_0)$  is normally obtained from suction-controlled oedometer tests. However, as a

302 first approximation, it can be estimated from a conventional eodometer test, maintaining the water content

303 of the sample constant to avoid drying as much as possible.

304 According to Eq. (1),  $\varepsilon_v(\sigma_{vf}, \Delta\Psi)$ , can be calculated as follows:

305

306  $\varepsilon_v(\sigma_{vf}, \Delta\Psi) = I_{pt}(\sigma_{vf}) \cdot \log\left(\frac{\Psi_f}{\Psi_0}\right)$  (10)

307 The volumetric strain will be swelling when  $I_{pt} > 0$  and  $\Psi_f < \Psi_0$

308 There will be shrinkage when  $I_{pt} > 0$  and  $\Psi_f > \Psi_0$

309 The volumetric strain will be collapse when  $I_{pt} < 0$  and  $\Psi_f < \Psi_0$

310

311 Substituting Eq. (8) into this expression, we obtain:

312

313  $\varepsilon_v(\sigma_{vf}, \Delta\Psi) = C \log\left(\frac{p_s}{\sigma_{vf}}\right) \cdot \log\left(\frac{\Psi_f}{\Psi_0}\right)$  (11)

314

315 Thus, the expression to calculate the volumetric deformation (under oedometric conditions) of the

316 Guadalquivir blue marl in the range of suctions between the swelling ( $\Psi_{sw}$ ) and the shrinking limit ( $\Psi_{sh}$ ) is

317 obtained substituting Eq. (11) into Eq. (9):

318

319 
$$\varepsilon_v(\Delta\sigma_v, \Delta\Psi) = \varepsilon_v(\Delta\sigma_v, \Psi_0) + C \log\left(\frac{p_s}{\sigma_{vf}}\right) \cdot \log\left(\frac{\Psi_f}{\Psi_0}\right) \quad (12)$$

320

321 For suctions above  $\Psi_{sh}$ , the deformation is obtained substituting in Eq. (12) the value of suction  
322 corresponding to the shrink limit:

323

324 
$$\varepsilon_v(\Delta\sigma_v, \Delta\Psi) = \varepsilon_v(\Delta\sigma_v, \Psi_0) + C \log\left(\frac{p_s}{\sigma_{vf}}\right) \cdot \log\left(\frac{\Psi_{sh}}{\Psi_0}\right) \quad (13)$$

325

326 And, similarly, for suctions under  $\Psi_{sw}$ :

327

328 
$$\varepsilon_v(\Delta\sigma_v, \Delta\Psi) = \varepsilon_v(\Delta\sigma_v, \Psi_0) + C \log\left(\frac{p_s}{\sigma_{vf}}\right) \cdot \log\left(\frac{\Psi_{sw}}{\Psi_0}\right) \quad (14)$$

329

330 The practical application of this method to the case of the Guadalquivir blue marl requires as the input  
331 the initial and final values of the suction and vertical pressures ( $\sigma_v$ ,  $\sigma_{vf}$ ,  $\Psi_0$ ,  $\Psi_f$ ). The output provides the  
332 vertical deformation of the soil. In order to extend the model to other types of soils it would be necessary  
333 to estimate the instability index and the suctions corresponding to the swell and shrink limits ( $I_{pt}(\sigma_{vf})$ ,  $\Psi_{sw}$ ,  
334  $\Psi_{sh}$ ) with the method described in this paper or a similar method.

335 For validation purposes, the deformations from the suction-controlled oedometer tests have been  
336 compared with the values calculated with the proposed model. The results of the comparison are displayed  
337 graphically in Fig. 10 for two reference pressures (50 kPa and 400 kPa).

338 As can be seen, the volumetric deformation calculated with the proposed model approximates the  
339 experimental results from suction-controlled oedometer tests with an acceptable accuracy. Furthermore,  
340 its simplicity makes it very appropriate for use in geotechnical engineering applications.

341

## 342 Discussion

343 The model simulates swell, shrink and collapse behaviour of undisturbed samples at different conditions  
344 of vertical deformation and suction change under oedometric conditions.

345 For the range of suctions between the swell limit and the shrink limit, the relationship between  
346 volumetric strain and suction is linear. This is the trend deduced from the suction controlled tests carried  
347 out by Escario and Sáez (1973), Kassif et al. (1973), Justo et al. (1984), Richards (1984), Mitchell and

348 Avalle (1984), Delgado (1986) and McKeen (1992). According to Pile and McInnes (1984), based on  
349 volume change it might be expected that  $I_{pt}$  for the wetting-up test in the oedometer will be three times that  
350 for the drying test in samples without lateral restraint. In practice it has been found that the ratio is less than  
351 2, and apparently depends on the extent of small fissures in the fiels samples, which close up during  
352 oedometer testing.

353 For suctions outside of this range the soil deformations are nearly constant. This trend for low suctions  
354 and expansive soil is glimpsed in the paper by McKeen (1992), and for collapsing soils in the paper by  
355 Vázquez et al. (2013).

356 For a particular site (site A), the same equations have acceptably fitted the results corresponding to  
357 depths ranging from 6.6 to 21 m (Table 4). This is because, at this site, the scattering of the initial suction  
358  $\Psi_0$  was small and an average value of 850 kPa could be used without a loss of accuracy. The same assertion  
359 is true for the swell limit. When there are important differences in these and other parameters, it will be  
360 better to consider different layers in the calculation.

361 In this paper, the trends hinted in several papers have been collected in a single model. As can be seen  
362 in Figure 10, the volumetric deformation calculated with the proposed model approximates the  
363 experimental results from suction-controlled oedometer tests with an acceptable accuracy.

364

## 365 **Conclusions**

366 In this paper we analysed the volumetric behaviour under oedometric conditions of a high plasticity  
367 carbonate clay: the Guadalquivir blue marl. In relation to previous studies, this work contributes to a deeper  
368 understanding of the characteristics of this type of soil, especially of its deformational behaviour under  
369 suction and vertical pressure changes.

370 The blue marl forms the bedrock layer of the Guadalquivir river valley (Spain) and has been responsible  
371 for many accidents and much damage due to its high fragility, its expansive character and its vulnerability  
372 against moisture changes.

373 A comprehensive test campaign has been conducted to determine the physical and chemical properties  
374 of the blue marl, that was classified as a high plasticity clay (CH) with a carbonate content above 25% and  
375 a high percentage of phyllosilicates, mainly illite and smectite. Analysis by scanning electron microscopy  
376 (SEM) and mercury intrusion porosimetry (MIP) allowed the characterising of its internal structure,

377 revealing clear differences between its macro and microstructure. The SWCC was obtained using a dew  
378 point psychrometer for suctions greater than 1 MPa and a pressure membrane apparatus for lower suctions.

379 To predict the deformational behaviour of this material, an empirical 1-D model has been proposed.  
380 The model simulates both the swell, shrink or collapse behaviour of undisturbed samples under different  
381 conditions of vertical loading and suction change. Currently, no simple model exists to predict the  
382 deformational behaviour of expansive soils that considers the range of strain, suction and vertical loading  
383 or the type of samples included in this paper.

384 The model is based on data from shrink-swell tests to characterise the relationship between deformation  
385 and suction change (in a logarithmic scale). It was found that for the range of suctions between the swell  
386 limit and the shrink limit this relationship is linear and the correlation ratio corresponds to the instability  
387 index ( $I_{pt}$ ), that has been related to the applied vertical pressure through a logarithmic expression (derived  
388 by the authors).

389 For suctions outside of this range the soil deformations remain nearly constant.

390 From the results of shrink-swell tests conducted on undisturbed samples, the average value of the shrink  
391 limit was found to be 5%, while the swell limit was 30%. These values did not depend on the depth of  
392 sample collection.

393 The proposed unidimensional model was compared with experimental data from suction-controlled  
394 oedometer tests performed on undisturbed samples. The results obtained with the proposed model showed  
395 an acceptable agreement with the measured data.

## 396 **Acknowledgements**

397 The authors would like to acknowledge the financial support from the Innovation and Science Office of the  
398 Regional Government of Andalusia (Project TEP-6632) and the Spanish Ministry of Science and  
399 Innovation (grant BIA2010-20377). The English correction has been financed with the help for  
400 internationalisation granted to the IUACC through the VI Plan of Research and Transference of the  
401 University of Seville.

## 402 **References**

403 Aitchison, G.D. (1973). "The quantitative description of the stress-deformation behaviour of expansive soil.  
404 Preface to set of papers". *Third International Conference on Expansive Soils*, Haifa, Vol. 2, pp. 79–82.

405 Alonso, E.E. and Gens, A. (2006a). "Aznaicóllar dam failure. Part 1: Field observations and material  
406 properties". *Géotechnique*, 56(3): 165-183.

407 Alonso, E.E. and Gens, A. (2006b). "Aznaicóllar dam failure. Part 3: Dynamics of the motion".  
408 *Géotechnique*, 56(3): 203-210.

409 Alonso, E.E., Gens, A. and Whight, D. (1989). "General report". *9<sup>th</sup> European Conf. on Soil mech. and*  
410 *Foundatio Eng. Groundwater Effects in Geotechnical Engineering*. Vol. 3. 1087-1146.

411 AS1289.7.1.1-1992 (1992). "Methods for Testing Soils for Engineering Purposes. Method 7.1.1:  
412 Determination of the Shrinkage Index of a Soil; Shrink Swell Index", *Standards Australia*.

413 ASTM D5298-94 (1994). "Standard test method for measurement of soil potential (suction) using filter  
414 paper". *Annual Book of ASTM Standards*, ASTM Intrenational, Philadelphia.

415 Bocking, K.A. and Fredlund, D.G. (1980). "Limitations of the axis translation technique". *IV International*  
416 *Conference on Expansive Soils*, Denver, 1:117–135.

417 Brasher, B.R., Franzmeier, D.P., Vallassi, V.T. and Davidson, S.E. (1966). "Use of Saran resin to coat  
418 natural soil clods for bulk density and water-retention measurements". *Soil. Sci.* pp 101:108.

419 Bulut, R., Hineidi, S.M. and Bailey, B. (2002). "Suction measurement filter paper and chilled mirror  
420 psychrometer". *Proc. of the Texas Section American Society of Civil Engineers, Fall Meeting, Waco, 2-*  
421 *5 October*.

422 Cameron, D.A. (1989). "Tests for Reactivity and Prediction of Ground Movement". *Civil Engineering*  
423 *Transactions, I.E. Aust.*, Vol. 3, pp 121–132.

424 Delgado, A. (1986). "Influencia de la trayectoria de las tensiones en el comportamiento de las arcillas  
425 expansivas y de los suelos colapsables en el laboratorio y en el terreno". *Ph. D. thesis*, University of  
426 Sevilla, Spain.

427 Dhowian, A.W. (1990). "Field performance of expansive shale formation". *J. of King Abdulaziz University.*  
428 *Engineering Sciences*, 2:165–82.

429 Fityus, S., Smith, D.W. (1998). "A simple model for the prediction of free surface movements in swelling  
430 clay profiles". *2nd Int. Conf. on Unsaturated Soils*, Beijing, China, pp 473-478.

431 Fityus, S.G., Cameron, D.A., Walsh, P.F., 2005. "The shrink swell test". *Geotech. Testing J.*, 28(1): 1-10.

432 Fredlund, D.G. (1983). "Prediction of ground movements in swelling clays". *31st Annual Soil Mech. and*  
433 *Found Eng. Conf.*. University of Minnesota, Minneapolis.

434 Fredlund, D.G., Pham, H.Q. (2006). "A volume-mass constitutive model for unsaturated soils in terms of  
435 two independent stress variables". *4th Int. Conf.on Unsaturated Soils*. ASCE, Carefree, Vol. 1, pp 105-  
436 134.

437 Galera, J.M., Checa, M., Pérez, C., Williams, B., Pozo, V., (2009). "Caracterización de detalle de las margas  
438 azules del Guadalquivir mediante ensayos in situ y de laboratorio". *Ingeopres*. 186: 16-22. ISSN 1136-  
439 4785.

440 Gee, G., Campbell, M., Campbell, G. (1992). "Rapid measurement of low soil potentials using a water  
441 activity meter". *Soil Sci. Soc. Am. J.* 56:1068–1070.

442 Gens, A., Alonso, E.E. (1992). "A framework for the behaviour of unsaturated expansive clays". *Can.*  
443 *Geotech. J.*, 29: 1013-1032.

444 Gens, A., Alonso, E.E. (2006). "Aznalcóllar dam failure. Part 2: Stability conditions and failure  
445 mechanism". *Géotechnique*, 56(3): 185-201.

446 Hamberg, D.J., Nelson, J.D. (1984). "Prediction of floor slab heave". *5th Int. Conf. on Expansive Soils*,  
447 Adelaide, South Australia, pp 137-140.

448 Hoffmann, C., Romero, E., Alonso, E.E. (2005). "Combining different controlled-suction techniques to  
449 study expansive clays". *Int. Symp. Advanced Exp. Unsat. Soil Mech.*. Trento. Italy.

450 Justo, J.L., Delgado, A., Ruiz, J. (1984). "The influence of stress-path in the collapse-swelling of soils at  
451 the laboratory". *5th Int. Conf. on Expansive Soils*, Adelaide, South Australia, pp 67-71.

452 Kassif, G., Baker, R. and Ovidia, Y. (1973). *3<sup>rd</sup> Int. Conf. Expansive Soils, 1: 201-208*.

453 Kodikara, J.K., Choi, X. (2006). "A simplified analytical model for desiccation cracking of clay layers in  
454 laboratory tests". *Fourth International Conference on Unsaturated Soils. Geotechnical Special*  
455 *Publication*, 147, pp 2558–2569.

456 Leong, E.C., Tripathy, S. and Rahardjo, H. (2003). "Total suction measurement of unsaturated soils with  
457 a device using the chilled-mirror dew-point technique". *Géotechnique*, 53(2):173-182.

458 Llorente Gómez, E. (1986). "Riesgos geológicos". *Instituto Geológico y Minero de España*, ISBN: 84-505-  
459 7599-0.

460 Lytton, R.L. (1977). "Foundations in expansive soils". *Numerical Methods in Geotechnical Engineering*.  
461 C.S. Desai and J.T. Christian, McGraw Hill, N. Y. pp 427 - 457.

462 McKeen, R.G. (1980). "Field Studies of Airport Pavements on Expansive Soils". *4th International*  
463 *Conference on Expansive Soils*, pp 242–261.

464 McKeen, R.G. (1992). "A Model for Predicting Expansive Soil Behaviour". *7th Int. Conf. on Expansive*  
465 *Soils*, Dallas, TX, Vol. 1, pp 1–6.

466 Mitchell, P.W., Avasle, D.L. (1984). "A Technique to Predict Expansive Soil Movements". *5th Int. Conf.*  
467 *on Expansive Soils*, Adelaide, South Australia, pp 124–130.

468 Pile, K.C., McInnes, D.B. (1984). "Laboratory technology for measuring properties of expansive clays).  
469 *5th Int. Conf. on Expansive Soils*, Adelaide, South Australia, pp 85-93.

470 Pousada, E. (1984). "Deformabilidad de la arcillas expansivas bajo succión controlada". Centro de Estudios  
471 y Experimentación de Obras Públicas. CEDEX. Madrid. ISBN: 84-398-2554-4.

472 Puppala, A.J., Manosuthikij, T., Chittoori, B.C.S. (2014). "Swell and shrinkage strain prediction models  
473 for expansive clays". *Eng. Geology*, 168:1-8.

474 Richards, L.A. (1941). "A pressure-membrane extraction apparatus for soil solution". *Soil Sci.*, 51:377–  
475 386.

476 Richards, B.G. (1984). "Finite element analysis of volume change in expansive clays". *5th Int. Conf. on*  
477 *Expansive Soils*, Adelaide, South Australia, pp 141-148.

478 Tang, A.M., Cui, Y.J. (2005). "Controlling suction by the vapour equilibrium technique at different  
479 temperatures and its application in determining the water retention properties of MX80 clay". *Can.*  
480 *Geotech. J.*, 42: 287-296.

481 Tsige, M. (1999). "Microfábrica y mineralogía de las arcillas azules del Guadalquivir: influencia en su  
482 comportamiento geotécnico". CEDEX. Ministerio de Fomento, Madrid. ISBN: 84-498-0426-4.

483 Tu, H., Vanapalli, S.K. (2016). "Prediction of the variation of swelling pressure and one-dimensional heave  
484 of expansive soils with respect to suction using the soil-water retention curve as a tool". *Can. Geotech.*  
485 *J.*, 53: 1213-1234.

486 UNE 103200:1993 (1993). "Determinación del contenido de los carbonatos en los suelos". Asociacion  
487 Española de Normalización y Certificación AENOR. Madrid.

488 UNE 103602:1996 (1996). "Ensayo para calcular la presión de hinchamiento de un suelo en edómetro".  
489 Asociacion Española de Normalización y Certificación AENOR. Madrid.

490 Van Genuchten, M.T. (1980). "A closed-form equation for predicting the hydraulic conductivity of  
491 unsaturated soils". *J. Soil Science Soc. of America*, 44: 892-898.

492 Vanapalli, S.K., Lu, L. (2012). "A state-of-the art review of 1-D heave prediction methods for expansive  
493 soils". *Int J. Geotech.Eng.*, Vol. 6: 15-45.

494 Vanapalli, S.K., Lu, L., Oh, W.T. (2010). "A simple technique for estimating the 1-D heave in expansive  
495 soils". *5th Int. Conf. Unsaturated Soils*, Barcelona, Spain. September 6-8, 2010. CRC Press, Vol. 2, pp  
496 1201-1207.

497 Vázquez, M., Justo, J.L., Durand, P. (2013). "A simplified model for collapse using suction controlled  
498 tests". *18th Int. Conf. on Soil Mechanics and Geotechnical Engineering*, Paris, France. 2-5 September,  
499 2013. Presses des Ponts, Vol. 1, pp 1203-1206.

500 Vázquez-Boza, M., Justo, J.L., Durand, P., Morales-Esteban, A. (2014). "Macro and microstructure of  
501 Guadalquivir blue marls in cyclic suction-controlled drying and wetting test". *6th Int. Conf. on*  
502 *Unsat. Soils*, Sydney, Australia. 2-4 July, 2014. CRC Press, Vol. 1, pp 727-732.

503 Villar, M.V. (2000). "Caracterización termo-hidro-mecánica de una bentonita de Cabo de Gata". Ph.D.  
504 Thesis, Universidad Complutense de Madrid. Madrid. Spain.

505 Zabala, F., Alonso, E.E. (2011). "Progressive failure of Aznalcóllar dam using the material point method".  
506 *Géotechnique*, 61(9): 795-808. doi: 10.1680/geot.9.P.134.

507

1 **Table 1.** Most widely known uni-dimensional models.

Model	Volumetric behaviour	Type of sample	Vertical pressures range (kPa)	Suction range
Fredlund (1983)	Swelling	Disturbed	7 to $p_s^{(1)}$	$\Psi_0^{(4)}$ to saturation
Hamberg and Nelson (1984)	Swelling Shrinkage	Disturbed Undisturbed	Not applied	$w_s$ to $w_p^{(3)}$
Dhowian (1990)	Swelling	Undisturbed	0 to $p_s$	$\Psi_0$ to saturation
Fityus and Smith (1998)	Swelling	Disturbed	$p'_f^{(2)}$	$\Psi_0$ to saturation
Vanapalli et al. (2010)	Swelling	Disturbed	$p'_f$	$\Psi_0$ to saturation
Puppala et al. (2013)	Swelling Shrinkage	Disturbed	Not applied	$\Psi_f^{(4)}$ to saturation

2

3

<sup>(1)</sup>  $p_s$ : Swelling pressure.

4

<sup>(2)</sup>  $p'_f$ : Effective pressure.

5

<sup>(3)</sup>  $w_s/w_p$ : Shrinkage and plastic limit.

6

<sup>(4)</sup>  $\Psi_0, \Psi_f$ : Initial and residual suction.

7

8

9

10

11

12

13

14

15

16

17

18

19

20

21

22

23

1 **Table 2.** Average results of the laboratory tests:  $\gamma_s$  – unit weight of solid particles-,  $\gamma_d$  – dry unit weight-  
 2 ,  $w$  – water content-,  $w_L$  –liquid limit and  $I_p$ –plasticity index-.

ASTM T200 (%)	Activity	$\gamma_s$ (kN/m <sup>3</sup> )	$\gamma_d$ (kN/m <sup>3</sup> )	$w$ (%)	$w_L$	$I_p$
98.2 ± 1.9	0.47	26.9 ± 0.5	15.9 ± 0.5	25.6 ± 1.8	58.2 ± 6.5	33.1 ± 3.7

3  
 4  
 5  
 6  
 7  
 8  
 9  
 10  
 11  
 12  
 13  
 14  
 15  
 16  
 17  
 18  
 19  
 20  
 21  
 22  
 23  
 24  
 25  
 26  
 27  
 28  
 29  
 30  
 31  
 32  
 33  
 34  
 35  
 36

1 **Table 3.** Average mineralogical composition of the Guadalquivir blue marls.

Phyllosilicates			Calcite (%)	Quartz (%)	Dolomite (%)
Smectite (%)	Illite (%)	Kaolinite (%)			
16.4 ± 14.7	18.4 ± 3.6	13.4 ± 4.3	32.8 ± 3.2	15.6 ± 4.3	3.4 ± 0.5

2  
3  
4  
5  
6  
7  
8  
9  
10  
11  
12  
13  
14  
15  
16  
17  
18  
19  
20  
21  
22  
23  
24  
25  
26  
27  
28  
29  
30  
31  
32  
33  
34  
35

1

**Table 4.** Experimental results for Shrink-Swell Test.

Depth of the sample (m)	$w_{sw}$ (%)	$w_{sh}$ (%)	$\varepsilon_{sw}$ (%)	$\varepsilon_{shver}$ (%)	$\varepsilon_{shver} / \varepsilon_{shvol}$
6.6	34.1	6.23	1.20	3.29	0.47
6.6	34.0	7.53	1.04	4.19	0.61
18	33.0	4.05	9.20	4.19	0.47
21	32.3	4.21	3.10	4.59	0.45
21	29.8	4.20	7.00	3.10	0.42

2  
3  
4  
5  
6  
7  
8  
9  
10  
11  
12  
13  
14  
15  
16  
17  
18  
19  
20  
21  
22  
23  
24  
25  
26  
27

1

**Table 5.** Empirical oedometer tests.

Test	Suction (kPa)	Saline solution	Vertical pressures Load/Unload (kPa)
EDO-SUC- 1	0	Saturation	10-50-100-200-400-800-1000-400-10
EDO-SUC- 2	100	NaCl	10-50-100-200-400-800-1000-400-10
EDO-SUC- 3	450	NaCl	10-50-100-200-400-800-1000-400-10
EDO-SUC- 4	850	NaCl	10-50-100-200-400-800-1000-400-10
EDO-SUC- 5	10000	NaCl	10-50-100-200-400-800-1000 400-10
EDO-SUC- 6	33100	NaCl	10-50-100-200-400-800-1000 400-10
EDO-SUC- 7	94200	CaCl <sub>2</sub>	10-50-100-200-400-800-1000 400-10

2

3

4

5

6

7

8

9

10

11

12

13

14

15

16

17

18

19

20

21

22

23

24

25

26

27

28

29

30

31

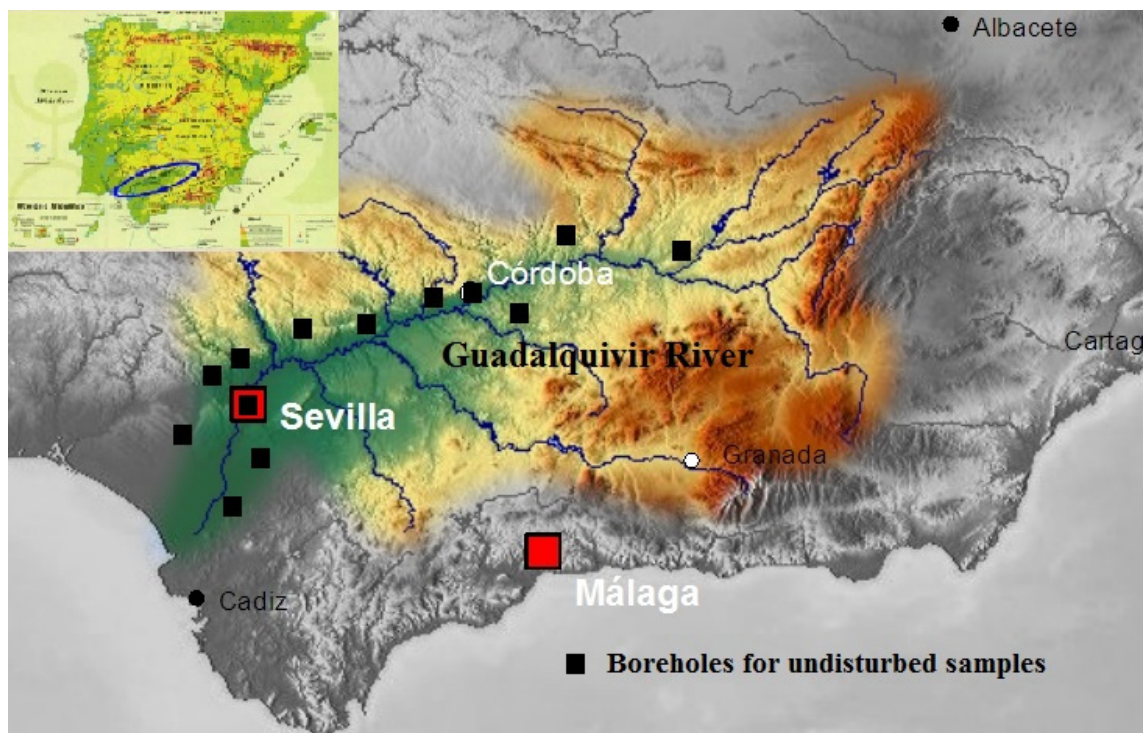
1

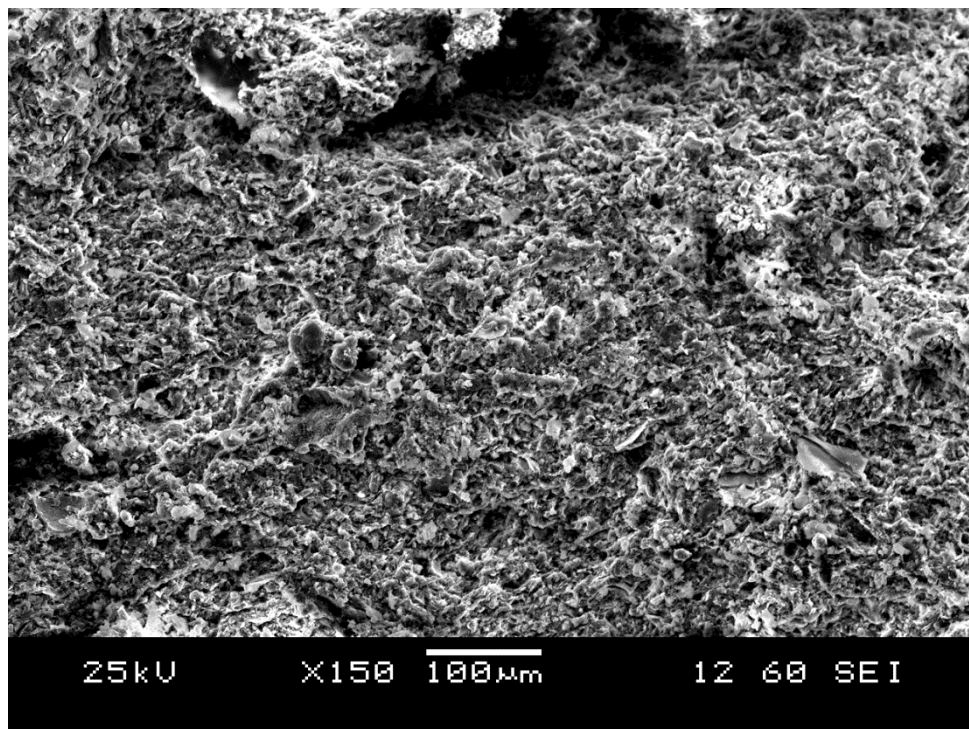
**Table 6.**  $I_{pt}$  variation with the vertical pressure ( $\sigma_v$ )

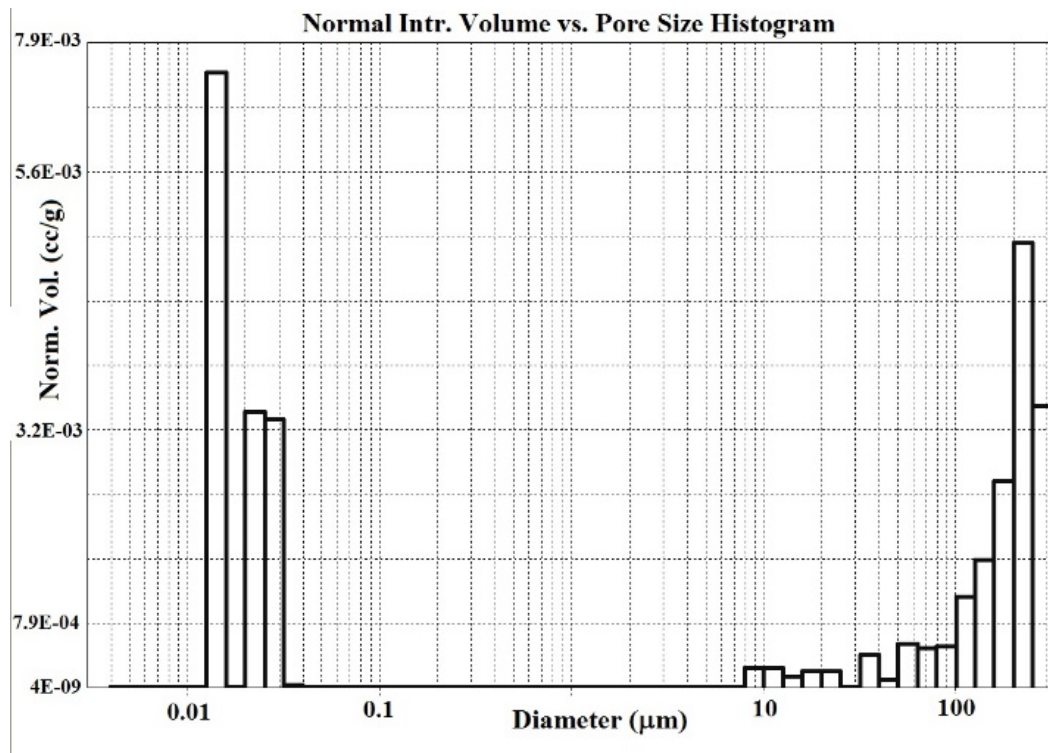
Vertical pressure $\sigma_v$ (kPa)	$I_{pt}$
10	0.021
50	0.014
100	0.007
400	-0.013
800	-0.024
1000	-0.021

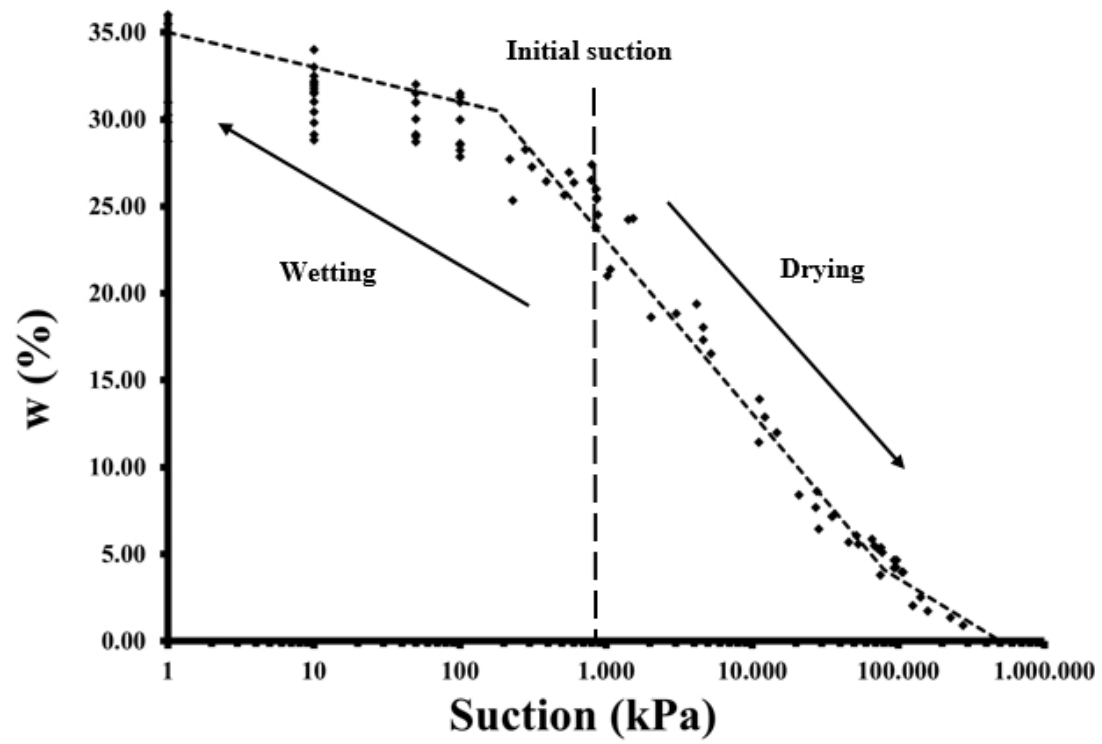
2

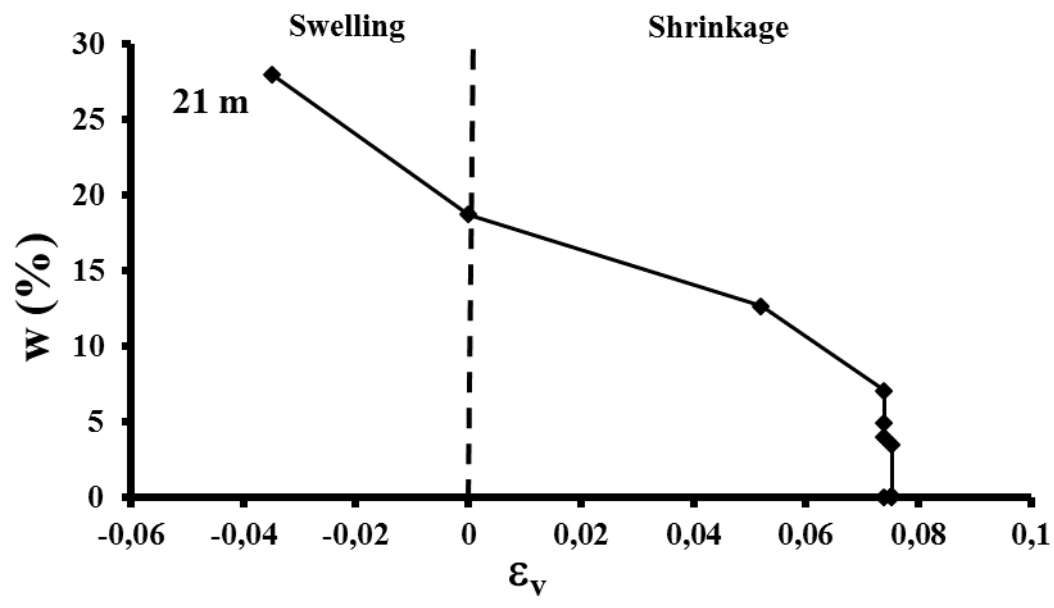
3

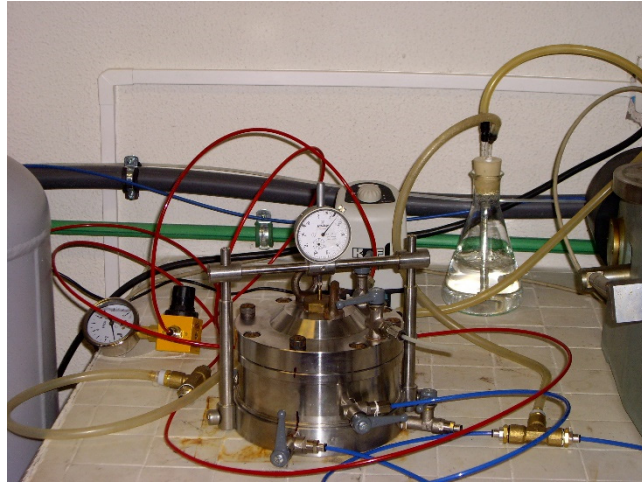


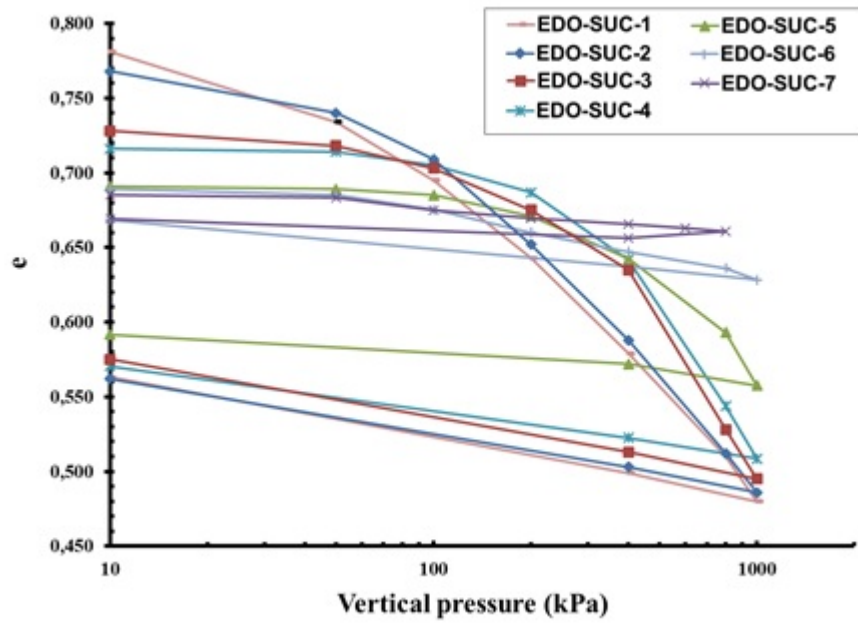


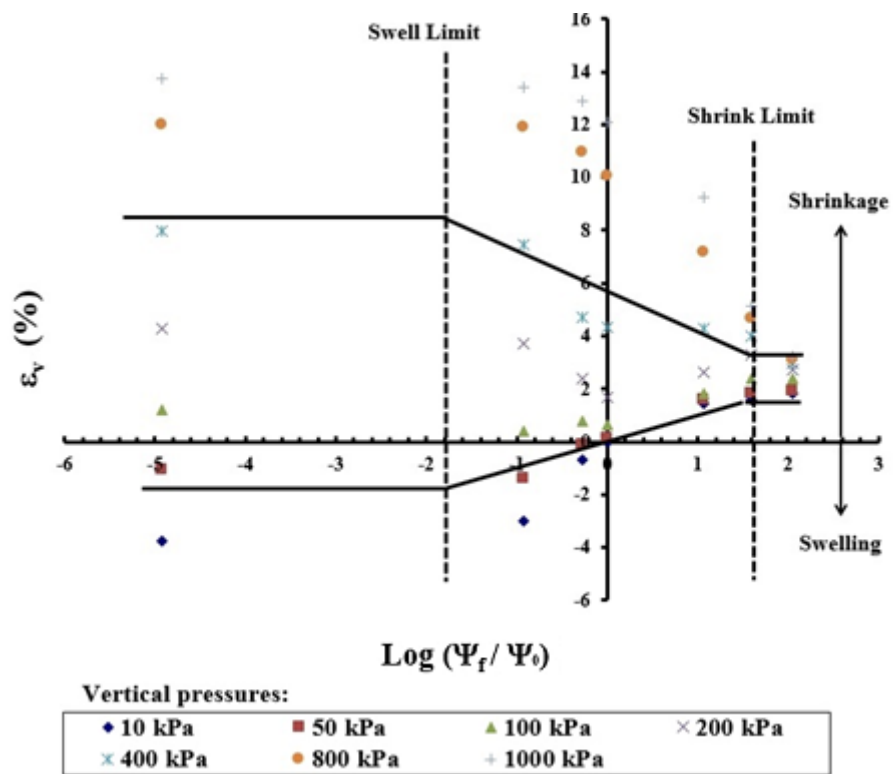


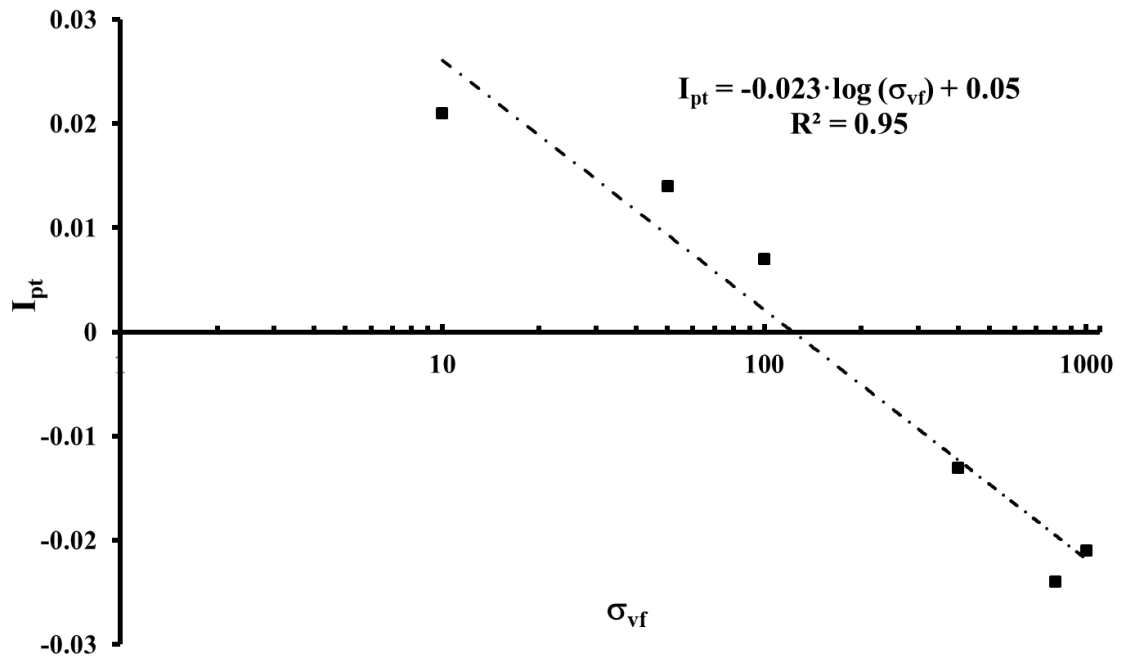




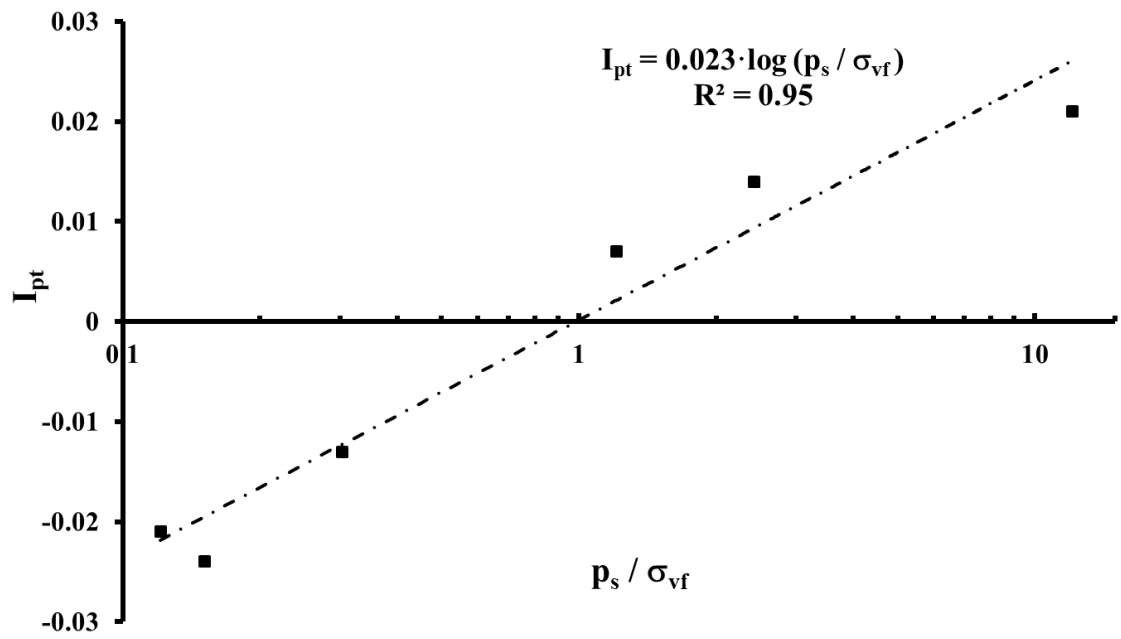




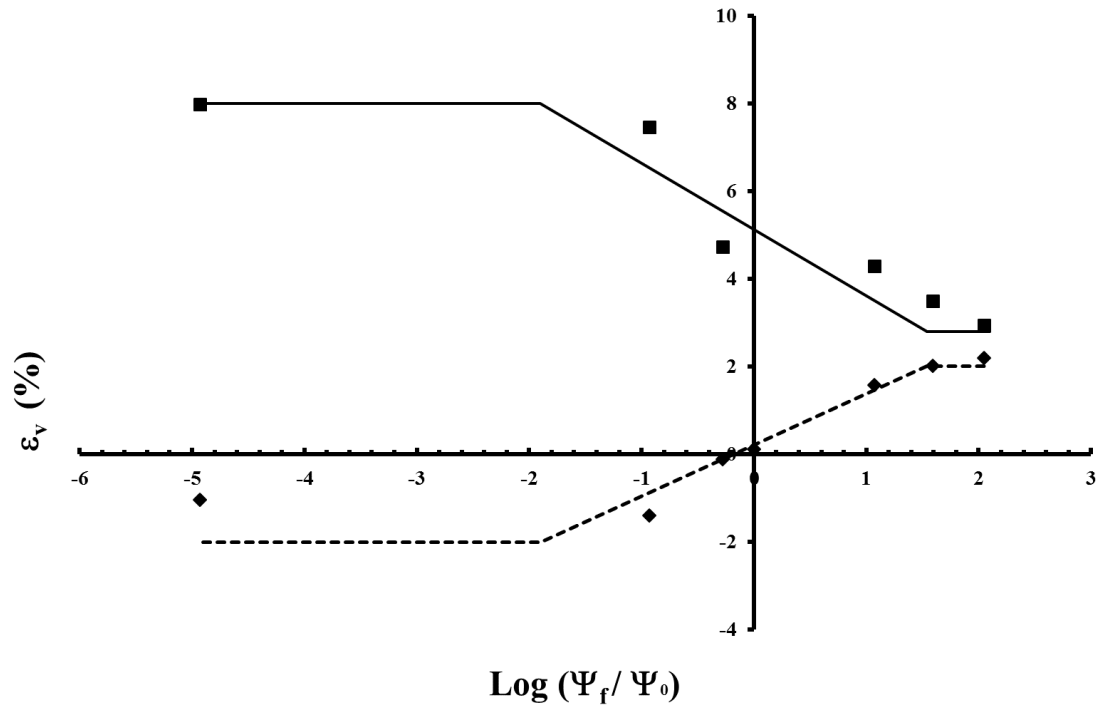




a)



b)



- ◆ Experimental results (vertical pressure: 50 kPa)
- Experimental results (vertical pressure: 400 kPa)
- Model (50 kPa)
- Model (400 kPa)

- 1       **Fig. 1.** Samples location.
- 2
- 3       **Fig. 2.** SEM picture.x150 zoom (Vázquez-Boza et al., 2014)
- 4
- 5       **Fig. 3.** MIP. Pore-size distribution before the suction-controlled tests were done (Vázquez-Boza et al.,
- 6       2014).
- 7
- 8       **Fig.4.** SWCC of the Guadalquivir blue marl.
- 9
- 10       **Fig. 5** Shrink-Swell test results. Depth of the sample 21 m.
- 11
- 12       **Fig.6** Suction-controlled oedometer cell (Vázquez-Boza et al., 2014).
- 13
- 14       **Fig. 7.** Oedometer tests results.
- 15
- 16       **Fig. 8** Volumetric deformation vs. suction for two vertical reference pressures (50 and 400 kPa).
- 17
- 18       **Fig. 9.** Correlations of  $I_{pt}$
- 19       a)  $I_{pt}$  as a function of  $\sigma_{vf}$
- 20       b)  $I_{pt}$  as a function of  $p_s/\sigma_{vf}$
- 21
- 22       **Fig. 10** Volumetric deformation vs. Suction for two vertical reference pressures.
- 23